ELSEVIER

Materials Science and Engineering B93 (2002) 55–59

MATERIALS SCIENCE & ENGINEERING B

www.elsevier.com/locate/mseb

Localization effects in InGaAsN multi-quantum well structures

A. Hoffmann [a,*], R. Heitz [a], A. Kaschner [a], T. Lüttgert [a], H. Born [a], A.Y. Egorov [b,1], H. Riechert [b]

[a] *Institut für Festkörperphysik, Technische Universität Berlin, Hardenbergstrasse 36, D-10623 Berlin, Germany*
[b] *Infineon Technologies, Corporate Research, CPR 7, 81730 Munich, Germany*

Abstract

The optical properties of InGaAsN/GaAs multiple quantum wells were investigated as a function of the nitrogen molar fraction. Time-integrated and time-resolved photoluminescence investigations demonstrate that localization effects at potential fluctuations play an important role in understanding the exciton dynamics. The results are supported by temperature-dependent photoluminescence and photoluminescence excitation investigations. In the last part, the state of the art of the 1.3 μm laser development is overviewed.

Keywords: InGaAsN; Photoluminescence; Exciton dynamics

1. Introduction

InGaAsN is considered a promising material for laser devices working at 1.3 or 1.5 μm. Incorporation of In and N into GaAs results in a strong redshift of the emission wavelength. Furthermore, the opposite effect of In and N on the lattice constant enables lattice-matching of InGaAsN on GaAs [1,2]. Most attractive is the realization of 1.3 μm vertical cavity surface emitting lasers (VCSELs) on GaAs using the well-established AlAs/GaAs distributed Bragg reflector (DBR) techniques [3,4]. Unfortunately, however, an increasing nitrogen content often reduces the luminescence efficiency, and so the laser threshold grows up [5,6]. It may be an intrinsic property of the alloy or due to nitrogen clustering in InGaAs [7,8]. In the photoluminescence (PL) spectra, these kind of potential fluctuations appear in terms of localization effects, e.g. affecting the exciton fine structure [9]. The purpose of the paper is to investigate the optical and structural properties of multi-quantum well (MQW) structures with varying nitrogen content and corresponding laser structures. Time-integrated and time-resolved PL (TRPL) and PL excitation spectroscopy (PLE) are used to elucidate the radiative and non-radiative processes in these MQW heterostructures.

2. Experimental

All samples were grown by solid source molecular beam epitaxy (MBE) on GaAs(001) substrates in As-rich growth conditions. A radio frequency coupled plasma source was used to create reactive nitrogen radicals from N_2. All samples contain eight 4 nm thick InGaAsN quantum wells with nitrogen concentrations of 1.5, 1.9, 2.3, and 2.6% and are capped with 10 nm GaAs. The concentrations have been estimated from X-ray diffraction data. An In molar fraction of 37% was chosen to achieve type I band. Details are given in Ref. [10]. Time-integrated PL spectra were recorded with a tungsten lamp dispersed by a double-grating monochromator as the excitation source and a cooled Ge-diode for detection. TRPL measurements were carried out under a Ti–sapphire laser system tuned to 790 nm exciting above the band gap of GaAs. For resonant investigations picosecond (ps)-pulses of an optical parametric oscillator pumped by a ps-Ti–sapphire laser were used. The luminescence was dispersed by a subtractive double-grating monochromator and detected with a multi-channel plate photomultiplier with an S1-cathode in photon-counting mode. The system

* Corresponding author. Tel.: +49-30-31422001; fax: +49-30-31422064.
E-mail address: axel0431@mailszrz.zrz.tu-berlin.de (A. Hoffmann).
[1] On leave from the A.F. Ioffe Physico Technical Institute, St. Petersburg, Russia.

0921-5107/02/$ - see front matter
PII: S0921-5107(02)00044-2

response with a full width at half maximum (FWHM) of ~20 ps was taken into account in the analysis of the transients using convolution techniques.

3. Optical properties of GaAsN and InGaAsN

The influence of the nitrogen mole fraction on the band gap of tensile-strained GaAsN (circles) and strain-compensated InGaAsN (triangles) alloys, which are lattice-matched to GaAs at 300 K, is shown in Fig. 1(a). The incorporation of 1% nitrogen reduces the energy gap E_G by ~150 meV. Additional incorporation of In shifts the band gap further to longer wavelengths. InGaAsN is lattice-matched to GaAs for an In/N ratio of ~3. The bowing parameter of the GaAs–GaN material system was estimated from the earlier described curve for the tensile-strained dilute GaAsN alloy and is presented in Fig. 1(b). The bowing parameter starts at ~25 eV and decreases rapidly with increasing nitrogen content. For a nitrogen mole fraction of 3.45%, the bowing parameter can be estimated as 12.5 eV. The focus of this work is on the investigation and understanding of the optical properties of multiple quantum wells based on the incorporation of nitrogen in GaAs. In Fig. 2, the room temperature transition energy is shown as a function of the quantum well thickness. The luminescence of a 4 nm thick InGaAsN MQW varies between 1.1 eV (1.5% N) and 1.02 eV (2.6% N) with FWHMs of 30 and 58 meV, respectively.

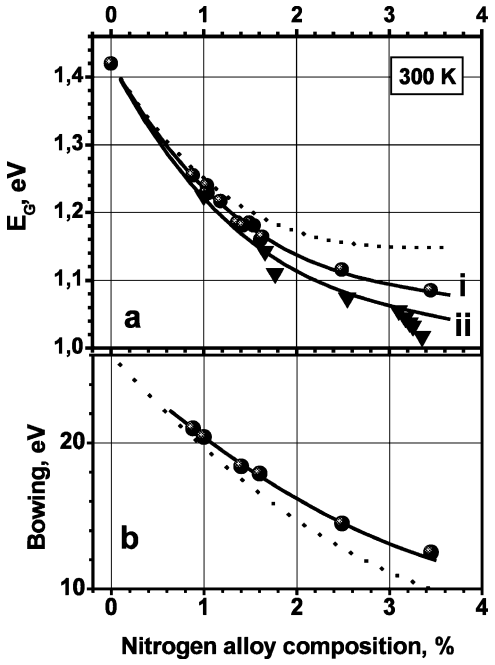

Fig. 1. (a) Band gap energy for tensile-strained GaAsN alloys on GaAs (circles), and for InGaAsN strain compensated alloys (triangles) as function of the nitrogen content. (b) Bowing parameter of the band gap of tensile-strained dilute GaAsN alloys [3].

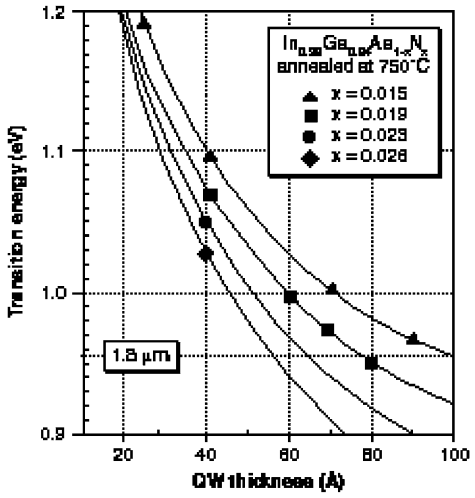

Fig. 2. Ground state transition energy (300 K) for InGaAsN/GaAs QWs depending on the QW thickness and composition. Experimental data (symbols) determined by PL [3].

In Fig. 3, helium temperature luminescence spectra of 4 nm thick InGaAsN MQWs as a function of the nitrogen content are seen. As expected, the InGaAsN luminescence is shifted to longer wavelengths with increasing nitrogen content. The origin of the 1.35 eV luminescence band is an open question. The luminescence band occurs in all investigated MQW samples, though the intensity is 10–100 times smaller than the InGaAsN MQW luminescence band. The transition energy shows no clear correlation to the nitrogen content. Additional information obtained from Fig. 4 exhibits excitation spectra of the InGaAsN MQW luminescence with 1.5% nitrogen content and of the

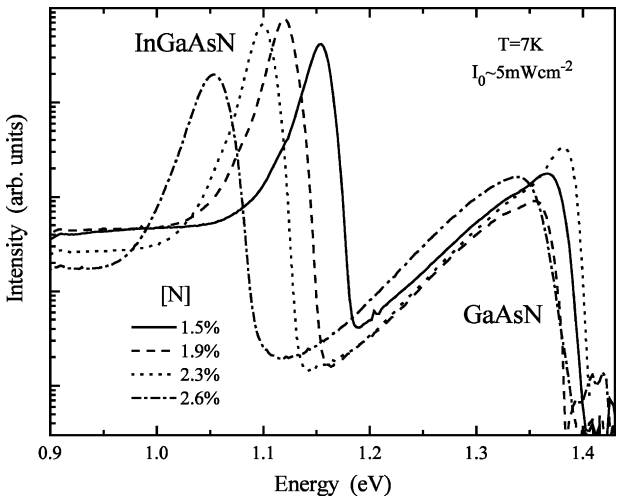

Fig. 3. Luminescence spectra of In GaAsN MQWs as a function of the nitrogen content.

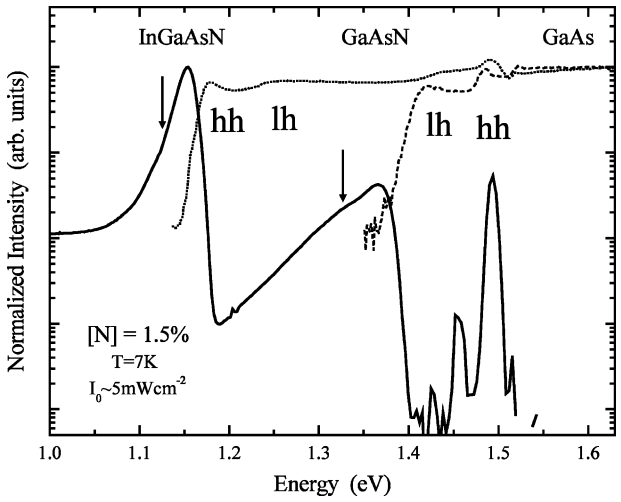

Fig. 4. PL excitation spectra of the InGaAsN MQW luminescence and the 1.35 eV band.

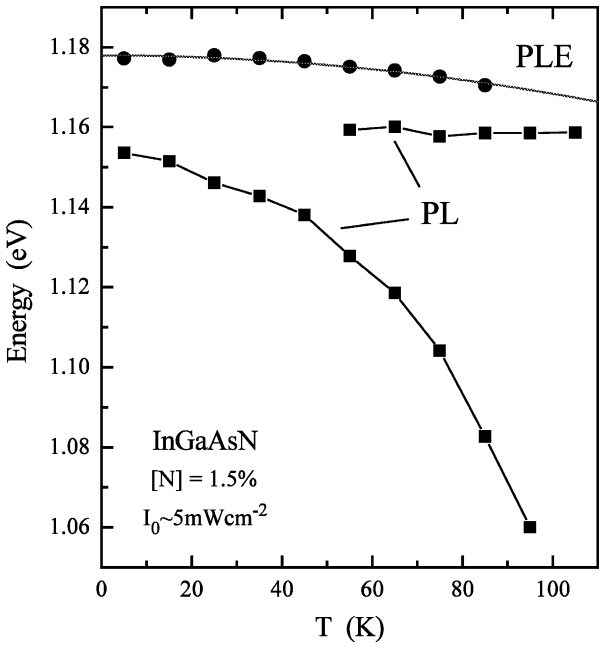

Fig. 5. Shifts of the PLE and PL maxima of the InGaAsN MQW as a function of temperature. The nitrogen content amounts to 1.5%.

1.35 eV band, which are representative for all samples. Both bands show excitation spectra, where a doublet of excitation lines appears. The two excitation maxima of the MQW luminescence can be explained by the splitting of the light (lh)- and heavy (hh)-hole exciton of the MQW indicating a compressive strain. On one hand, the lh–hh splitting of the doublet in the excitation spectrum of the 1.35 eV band is reversed, suggesting the underlying structure to be tensile strained. On the other hand, high-resolution transmission electron microscopy (HRTEM) suggests a nitrogen content of $\sim$1.5% outside of the 4 nm MQW [11]. The formation of GaAsN is a result of the MBE growth procedure, in particular of how the In and N flux are switched on. Consequently, we attribute the 1.35 eV band to the tensile-strained GaAsN alloy. Furthermore, the PLE spectra reveal transfer processes from the InGaAs alloy to the InGaAs MQW. The lh–hh splitting of the excitons in the MQW allows to estimate the band offsets. These are different from those we reported in Ref. [12] because the authors have assumed the excitation maxima around 1.4 eV to be an excited state transition of the MQW. Our results show that this luminescence band results from the GaAsN alloy.

Additionally, from the PL and PLE spectra of the InGaAsN MQW luminescence the Stokes shifts as a function of the nitrogen content were determined. Increasing the nitrogen content from 1.5 to 2.6%, the Stokes shift grows from 20 to 60 meV. This shows that localization effects play an important role in the InGaAsN MQWs. Varying the excitation density from 0.3 W cm^{-2} to 300 kW cm^{-2}, the MQW band shifts $\sim$ 7 meV to higher photon energies. Time-delayed measurements show no redshift with increasing time, denoting that piezoelectric fields, if existent, are very weak. Thus, the earlier mentioned blueshift can be explained by band-filling effects. Therefore, in Fig. 5, temperature-dependent investigations of the MQW PL and PLE are shown. With increasing temperature, the energy of the PL maximum shows an S-shape-like behavior indicating a transition between recombination from localized and delocalized states. The temperature dependence of the band gap as given by the behavior of the MQW absorption in the PLE spectra is well described by Varshni's formula [13] (gray line). The anomalous temperature-induced shift of the emission energy is attributed to localization-induced tail states in the density of states [14,15]. Between 4 and 100 K a redshift appears, because on one hand the excitons gain sufficient thermal energy to overcome small potential barriers and become trapped in adjacent lower-energy levels before they recombine. On the other hand, the jump of the PL energy by 15 meV to higher energies is attributed to the thermal population of abundant higher-energy states, i.e. the blueshift indicates the transition from zero-dimensional to quantum well-like behavior. At higher temperatures, the temperature shift of the emission is mainly determined by the behavior of the band gap. Compositional and structural inhomogeneities such as fluctuations in the alloy composition and well thickness may account for the described band-tail states. The fact that these band-tail states are important for dynamical recombination can be seen in Fig. 6. The figure shows as an example the time-integrated PL of the InGaAsN MQW with a nitrogen content of 2.6% at 2 K and the decay and rise times obtained from fits of transients recorded at various

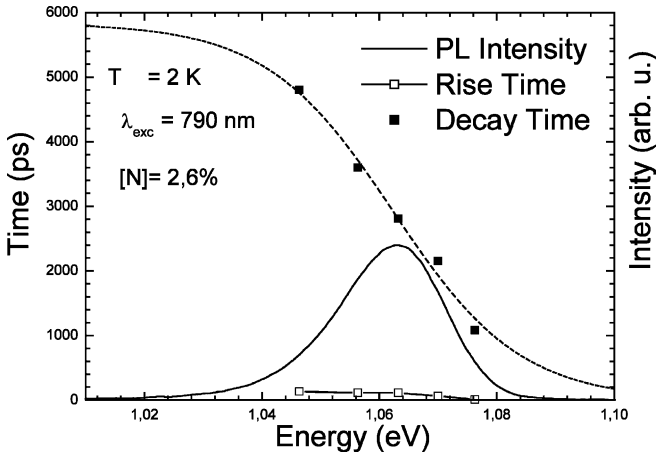

Fig. 6. Time-integrated PL of the InGaAsN MQW with 2.6% nitrogen content. The decay and rise times as functions of the detection energy recorded at 2 K. Eq. (1) was applied to determine the parameters $\tau_{rad} = 5800$ ps, $E_{me} = 1.078$ eV and $E_0 = 10.6$ meV.

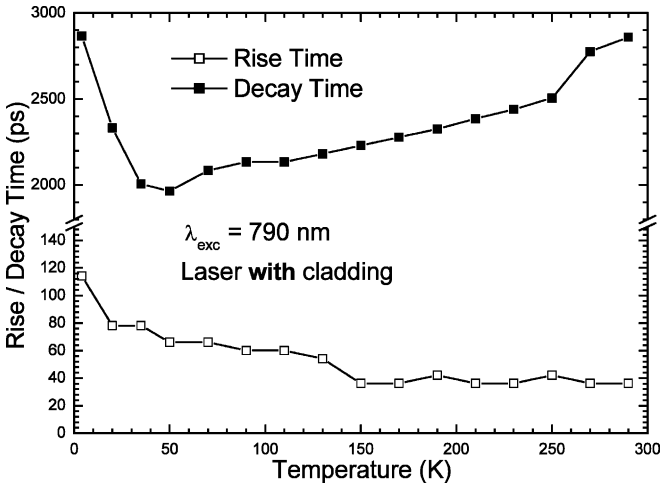

Fig. 7. Decay and rise times of an InGaAsN MQW laser structure as functions of temperatures.

detection energies. Generally, both the rise (130–20 ps) and decay (4800–400 ps) times decrease with increasing energy (1.04–1.075 eV). The rise time is determined by how fast the excitons can relax into the states where they recombine. In this experiment, we do not excite resonantly into the MQW but generate carriers in the GaAs barrier, which, however, explains only in part the relatively long rise time. In resonant time-resolved experiments, we observe the following main features; the rise times increase with decreasing excitation energies and the decay times increase at higher excitation energy with decreasing detection energy. This behavior is typical for capture and recapture processes between different localized states. Three different processes account for the decay of localized excitons: radiative and non-radiative recombinations as well as transfer processes. To determine the radiative lifetime of localized excitons as well as their average binding energy and mobility properties, we evaluated the results with a model introduced by Gourdon and Lavaillard [16] accounting for lateral energy transfer between localized states. Assuming the density of tail states to be proportional to $\exp(-E/E_0)$, the PL decay time for localized excitons as a function of the spectral position is determined by:

$$\tau(E) = \frac{\tau_{rad}}{1 + \exp[(E - E_{me})/E_0]} \quad (1)$$

where τ_{rad} is the radiative lifetime, E_{me} is the energy for which the radiative lifetime equals the lateral transfer time and E_0 is a characteristic energy for the density of states. The underlying model presumes that excitons transfer to lower-energy localized states by tunneling. A least-square-fit with Eq. (1) (dashed line in Fig. 6) yields the following parameters for the earlier mentioned MQW. For the MQW with 1.5 and 2.6% nitrogen content, $\tau_{rad} = 1800$ and 5800 ps, $E_{me} = 1.165$ and 1.078 eV and $E_0 = 6$ and 10.6 meV, respectively. This shows that at low temperatures the radiative lifetime increases with increasing nitrogen content. At room temperatures, the decay time increases (510–760 ps) with increasing nitrogen content of up to 2.3%. The decay time for the MQW sample with 2.6% is 185 ps. This can be explained with a higher defect concentration in this sample, since increasing nitrogen concentration, thus, leads to a stronger influence on defect-related non-radiative processes. HRTEM investigations show that in as-grown MQW structures the In content of the quantum fluctuates. The homogeneity of the QWL can be increased by annealing the sample at 750 K, however, on the cost of out-diffusion of nitrogen to the interfaces of the QWL.

4. Laser application

The active region of the lasers are based on 4 nm thick InGaAsN MQW heterostructures, which are symmetrically inserted into a 300 nm thick, undoped GaAs cavity. The p- and n-type cladding layers consist of 1.5 μm thick $Al_{0.35}Ga_{0.65}As$ doped with Be and Si to $1–6 \times 10^{17}$ and $5–9 \times 10^{17}$ cm^{-3}, respectively. The 0.6 μm thick GaAs contact layer is doped to about 1×10^{19} cm^{-3} in the top 200 nm. A typical result of TRPL investigations of such a laser structure is shown in Fig. 7 as a function of temperature. The decay time of 2800 ps at low temperatures decreases to 2000 ps at 50 K and increases again to 2600 ps at room temperature. The rise time decreases from 110 to 40 ps with increasing

temperatures. Additionally, we have measured temperature dependence of the PL. Taking into account the decrease of the PL intensity with increasing temperatures, the radiative and non-radiative lifetime are estimated from the observed decay times. Typical 4 and 300 K values are $\tau_{rad} = 3$ and 27 ns and $\tau_{non\text{-}rad} = 60$ and 6 ns, respectively. This shows that at room temperature the non-radiative processes in the laser structures are reduced, which is important for laser applications.

In the following, the state of the art of InGaAsN lasers for the 1.3 μm wavelength region is summarized. A comprehensive review is given in Ref. [3]. The characteristics of broad area lasers measured in a pulsed operation (pulse width $\tau = 2$ μs and repetition frequency $f = 5$ kHz) are a threshold current density of 0.5 kA cm^{-2}, a laser wavelength of 1.295 μm, and a T_0 of 60 K. Typical data for ridge-waveguide lasers are threshold currents of 16 mA, laser wavelengths around 1.295 μm, and T_0 of 80 K. VCSELs based on InGaAsN MQWs emit in cw operation at 1.305 μm till 80 °C, providing an output power of 1 mW at 25 °C. The lifetime of such lasers exceeds 3000 h. These data are comparable to those of the best InAs quantum dot lasers.

In conclusion, the characteristics of InGaAsN alloys and MQWs were investigated for nitrogen contents up to 3%. The dynamical behavior of the MQW structures shows a zero-dimensional character at low temperatures and a two-dimensional character at room temperature. It can be described through localized excitons at potential fluctuations. The responsible dynamical mechanisms of the InGaAsN laser structures at room temperatures are described mainly by radiative processes. The lasers at 1.3 μm demonstrate low-threshold current and high-power operation.

Acknowledgements

A.K. acknowledges the support of an Ernst-von-Siemens-scholarship. Part of this work was supported by Deutsche Forschungsgemeinschaft (SFB 296).

References

[1] M. Kondow, T. Kitatani, S. Nakatsuka, M.C. Larson, K. Nakahara, Y. Yazawa, K. Uomi, IEEE J. Sel. Topics Quantum Electron. 3 (1997) 719.
[2] W. Sham, W. Waluskiewicz, J.W. Anger, E.E. Haller, J.F. Geisz, D.J. Friedmann, J.M. Olsen, S.R. Kurtz, Phys. Rev. Lett. 82 (1999) 1221.
[3] H. Riechert, A. Yu Egorov, B. Borchert, S. Illek, Compound Semiconductor 6 (July 2001), cover story.
[4] K.D. Choquette, J.F. Klem, A.J. Fischer, O. Blum, A.A. Allermann, I.J. Fritz, S.R. Kurtz, W.G. Breitland, R. Sieg, K.M. Geib, J.W. Scott, R.I. Naone, Electron. Lett. 36 (2000) 1384.
[5] F. Hohnsdorf, J. Koch, S. Leu, W. Stolz, B. Borchert, M. Druminski, Electron. Lett. 35 (1999) 571.
[6] S. Sato, S. Satoh, Electron. Lett. 35 (1999) 1251.
[7] R.A. Mair, J.Y. Lin, H.X. Jiang, E.D. Johnes, A.A. Alleman, S.R. Kurtz, Appl. Phys. Lett. 76 (2000) 2241.
[8] J. Neugebauer, C.G. Van De Valle, Phys. Rev. B51 (1995) 10568.
[9] A. Kaschner, T. Lüttgert, H. Born, A. Hoffmann, A. Yu Egorov, H. Riechert, Appl. Phys. Lett. 78 (2001) 1391.
[10] A. Yu Egorov, D. Bernklau, D. Livshits, V. Ustinov, Zh.I. Alferov, H. Riechert, Electron. Lett. 35 (1999) 1643.
[11] V. Grillo, M. Albrecht, V.P. Strunk, A. Yu Egorov, H. Riechert, International Conference on Nitride Semiconductors 4, Denver (USA), July 2001, Phys. Status Solidi (2002), in press.
[12] M. Hetterich, M.D. Dawson, Appl. Phys. Lett. 76 (2000) 1030.
[13] Y.P. Varshni, Physica (Netherlands) 34 (1967) 149.
[14] L. Bergmann, M. Datta, M.A. Stroscio, S.M. Komirenko, R.J. Nemanich, C.J. Eitling, D.J.H. Lambert, H.K. Kwon, R.D. Depuis, Appl. Phys. Lett. 76 (2000) 1969.
[15] P.G. Eliseev, P. Perlin, J. Lee, M. Osinski, Appl. Phys. Lett. 71 (1997) 569.
[16] C. Gourdon, P. Lavaillard, Phys. status Solidi B153 (1989) 641.